Epidemics 5 (2013) 197–207

Contents lists available at ScienceDirect

Epidemics

journal homepage: www.elsevier.com/locate/epidemics

Examining rainfall and cholera dynamics in Haiti using statistical and dynamic modeling approaches

Marisa C. Eisenberg[a,b,c,*], Gregory Kujbida[d], Ashleigh R. Tuite[d], David N. Fisman[d], Joseph H. Tien[a,e]

[a] Mathematical Biosciences Institute, The Ohio State University, United States
[b] Department of Epidemiology, School of Public Health, University of Michigan, Ann Arbor, United States
[c] Department of Mathematics, University of Michigan, Ann Arbor, United States
[d] Dalla Lana School of Public Health, University of Toronto, Canada
[e] Department of Mathematics, The Ohio State University, United States

ARTICLE INFO

Article history:
Received 24 December 2012
Received in revised form
24 September 2013
Accepted 26 September 2013
Available online 21 October 2013

Keywords:
Cholera
Mathematical modeling
Waterborne diseases
Rainfall
Haiti

ABSTRACT

Haiti has been in the midst of a cholera epidemic since October 2010. Rainfall is thought to be associated with cholera here, but this relationship has only begun to be quantitatively examined. In this paper, we quantitatively examine the link between rainfall and cholera in Haiti for several different settings (including urban, rural, and displaced person camps) and spatial scales, using a combination of statistical and dynamic models.

Statistical analysis of the lagged relationship between rainfall and cholera incidence was conducted using case crossover analysis and distributed lag nonlinear models. Dynamic models consisted of compartmental differential equation models including direct (fast) and indirect (delayed) disease transmission, where indirect transmission was forced by empirical rainfall data. Data sources include cholera case and hospitalization time series from the Haitian Ministry of Public Health, the United Nations Water, Sanitation and Health Cluster, International Organization for Migration, and Hôpital Albert Schweitzer. Rainfall data was obtained from rain gauges from the U.S. Geological Survey and Haiti Regeneration Initiative, and remote sensing rainfall data from the National Aeronautics and Space Administration Tropical Rainfall Measuring Mission.

A strong relationship between rainfall and cholera was found for all spatial scales and locations examined. Increased rainfall was significantly correlated with increased cholera incidence 4–7 days later. Forcing the dynamic models with rainfall data resulted in good fits to the cholera case data, and rainfall-based predictions from the dynamic models closely matched observed cholera cases. These models provide a tool for planning and managing the epidemic as it continues.

Introduction

Haiti has been in the grip of a cholera epidemic since October 2010. As of July 1, 2013, the Haitian Ministere de la Sante Publique et de la Population (MSPP) has reported 664,259 cases and 8169 deaths.[1] Much attention has been paid to the early stages of the epidemic, including the origin of the epidemic strain (Chin et al., 2011; Cravioto et al., 2011; Piarroux et al., 2011), and the continuing threat posed by cholera to the current health and welfare of Haitians is of paramount concern. Although research efforts have evaluated the impact of water treatment practices, hand washing, and diet in urban (Dunkle et al., 2011) and rural (O'Connor et al., 2011) settings on cholera risk, have assessed the burden of *Vibrio cholerae* in water and food sources (Hill et al., 2011), and have evaluated such intervention efforts as opening of cholera treatment centers, education campaigns, and building of latrines (De Rochars et al., 2011; Ernst et al., 2011), case counts continue to rise more than two years after the epidemic began.

As intervention efforts grapple with a disease which is rapidly becoming endemic, understanding the role of the physical environment, including rainfall at both short-term time scales, and at a seasonal level, in the spread of cholera is crucial. Anecdotally, it has been noted that cholera case counts, which had been declining, rose sharply with the onset of seasonal heavy rains in the spring of 2011 (Adams, 2012; Periago et al., 2012). A better understanding

* Corresponding author at: Department of Epidemiology, School of Public Health, University of Michigan, 1415 Washington Hts. Ann Arbor, 48109 United States. Tel.: +1 734 763 2991.
E-mail addresses: marisae@umich.edu (M.C. Eisenberg), gwkujbida@gmail.com (G. Kujbida), ashleigh.tuite@utoronto.ca (A.R. Tuite), david.fisman@utoronto.ca (D.N. Fisman), jtien@math.osu.edu (J.H. Tien).

[1] July 1 report from MSPP.

1755-4365/$ – see front matter © 2013 Elsevier B.V. All rights reserved.
http://dx.doi.org/10.1016/j.epidem.2013.09.004

of the role of the physical environment in general, and rainfall in particular, in cholera dynamics in Haiti may lead to both improvement in the ability to forecast disease incidence, and would also help inform disease control interventions. Rinaldo et al. (2012) include rainfall in a complex model of cholera in Haiti, involving more than 300 spatial locations and including movement of both people and water. We take a simpler approach here, using a combination of statistical models and basic dynamic models to examine the relationship between rainfall with cholera case data from several different settings and spatial scales. Previous models of cholera in Haiti and elsewhere have incorporated varying degrees of spatial structure (Tuite et al., 2011; Chao et al., 2011; Reiner et al., 2012; Rinaldo et al., 2012; Bertuzzo et al., 2010, 2011; Gatto et al., 2012). In this paper, neither the statistical nor the dynamic models include an explicit spatial component. This bare-bones approach is intended to allow the model to be focused on the role of rainfall.

Previous studies have examined the role of weather and rainfall on cholera dynamics in Haiti (Rinaldo et al., 2012) and there have been many previous examinations of these effects in countries other than Haiti (Reiner et al., 2012; Altizer et al., 2006; Constantin de Magny et al., 2008; Emch et al., 2008; Faruque et al., 2005; Fernandez et al., 2009; Hashizume et al., 2010; Koelle, 2009; Lipp et al., 2002; Longini et al., 2002; Pascual et al., 2000; Ruiz-Moreno et al., 2007). Most countries in which the influence of rainfall on cholera incidence has been studied experience endemic cholera. Haiti, by contrast, has been cholera free for the past century, with the pathogen introduced from elsewhere. Associations between rainfall and cholera risk in other countries have shown a range of effects, with both positive and negative correlations having been reported at time lags varying from weeks to months (Emch et al., 2008; Fernandez et al., 2009; Hashizume et al., 2008, 2010; Mendelsohn and Dawson, 2008; Ruiz-Moreno et al., 2007). This may reflect the variety of potential mechanisms whereby rainfall may alter cholera risk, including via flooding leading to raw sewage contamination of water sources (Hashizume et al., 2008; Ruiz-Moreno et al., 2007), increased rainfall leading to increased iron availability, which in turn improves *V. cholerae* survival and expression of cholera toxin (Faruque et al., 2005; Lipp et al., 2002), and decreased water levels leading to increased usage of existing water sources and thus increased risk of contamination and disease transmission (Lipp et al., 2002; Ruiz-Moreno et al., 2007). Ruiz-Moreno et al. (2007) suggest a dual role for rainfall and cholera, with both high and low rainfall leading to increased transmission through different mechanisms. This variation between studies emphasizes the need for quantitative examination of site-specific case and environmental data in order to understand cholera dynamics in a given region.

We examine the relationship between cholera and rainfall in Haiti using several different approaches, including both statistical models (distributed lag nonlinear models (Gasparrini et al., 2010) and case-crossover analysis (Maclure, 1991)) and dynamic models ("SIWR" model (Tien and Earn, 2010) forced by rainfall time series data). The statistical models we use are flexible in how rainfall at different time lags affect cholera incidence (Gasparrini et al., 2010), and controls for systematic differences between individuals for risk factors such as water treatment practices and access to improved sanitation (Fisman et al., 2005; Maclure, 1991). For our dynamic models, we force our differential equation models directly with empirical rainfall data. This approach is different than previous work which first estimates time-varying transmission rates from case data, and then compares these transmission rates with environmental data (Koelle et al., 2005). We find a strong relationship between rainfall and cholera incidence for all methods used and spatial scales examined. A larger goal is to develop predictive models for cholera in Haiti on both the short and long term. Our dynamic models are promising for use in this regard – we present results on this below.

Data sets

We present here case data from several different sources (locations are shown in Fig. 1): MSPP data at the country-wide, Department (Sud), and city (Port-au-Prince) levels, cholera cases seen at Hôpital Albert Schweitzer (HAS), originating from four communes in a rural area of the Artibonite Department, and data from oral rehydration posts (ORPs) located in internally displaced persons camps (IDPs). These data encompass a wide range of spatial scales, and include three distinct types of settings (urban/rural/IDP), each with their own unique challenges for dealing with cholera.

Case data

Hôpital Albert Schweitzer Data. Data for cholera patients treated at Hôpital Albert Schweitzer (Fig. 1, red circle) as part of the hospital's routine clinical practices were provided from October 17, 2010 through July 11, 2011, under IRB protocol 2011H0197 (Ohio State University) and REB protocol 27264 (U. Toronto). Hospital Albert Schweitzer (HAS) is located in Deschapelles, Artibonite, near the epicenter of the Haitian cholera outbreak along the Artibonite river (shown in blue in Fig. 1). HAS is one of the largest hospitals in Haiti, providing care for over 345,000 people living in their 610 square mile service area. In response to the cholera epidemic, HAS established a 6-tent cholera ward adjacent to the hospital (Ernst et al., 2011). Provided data include date of admission, gender, age, and home location. These data comprise 4,662 total cases from 4 different communes (Verrettes, Dessalines, Petite Riviere de l'Artibonite, and La Chapelle) within the Artibonite Department.

Internally Displaced Person (IDP) Camp Data. A large number of IDP camps were set up to house Haitians whose homes were destroyed by the January 2010 earthquake, primarily in the greater Port au Prince region (Fig. 1, red star). As of May 4, 2011, the United Nations (UN) Water and Sanitation Health Cluster (WASH Cluster) listed 1001 IDP camps distributed over 13 communes (Carrefour, Cite Soleil, Croix-des-Boquets, Delmas, Ganthier, Grand Goave, Gressier, Jacmel, Leogane, Petionville, Petit Goave, Port-au-Prince, and Tabarre). Oral rehydration posts (ORPs) were established in more than 140 IDPs in early 2011 in response to cholera affecting the camps. Weekly case counts from March 14, 2011 through July 4, 2011 for 112 ORPs in the Port-au-Prince area were provided by the WASH Cluster and the International Organization for Migration (IOM-Haiti).

Ministere de la Sante Publique et de la Population (MSPP) Data. MSPP cholera case data were obtained from the publicly availably MSPP website (Ministere de la Sante Publique et de la Population). Daily cholera cases ("cas vus") reported by the MSPP were analyzed nationally from November 20, 2010 to June 4, 2011, for the Sud Department from November 18, 2010 to December 26, 2011, and for Port-au-Prince from June 26, 2011 to October 23, 2011 (dates were dependent on the range of case and rainfall data available for the region).

Rainfall data

Rainfall data came from rain gauges operated by the U.S. Geological Survey and the Haiti Regeneration Initiative, as well as from satellite measurements through the NASA Tropical Rainfall Measuring Mission.

United States Geological Survey Rainfall Data. The U.S. Geological Survey (USGS) maintains rain gauges in the Morne Gentilehomme (U.S. Geological Survey) and Foret de Pins (U.S. Geological Survey)

Fig. 1. Map of Haiti showing departments and locations of case and rainfall data sources. Red star indicates Port au Prince, although the general Port au Prince metropolitan area extends further (approximately indicated by the shaded red ellipse). HAS is indicated by a red circle adjacent to the Artibonite River (shown in blue). Port a Piment is indicated by the blue circle in the Sud Department. Approximate location of USGS rain gauges southeast of Port au Prince is shown as a shaded blue circle, and the shaded blue square surrounding HAS indicates the region of area-averaged NASA precipitation data. (For interpretation of the references to color in this figure legend and text, the reader is referred to the web version of the article.)

regions of Haiti, southeast of Port au Prince (Fig. 1, shaded blue circle). Weekly precipitation data were available from March 14, 2011 through November 6, 2011 for Morne Gentilehomme, and July 3, 2011 through November 6, 2011 for Foret de Pins.

Haiti Regeneration Initiative Data. Daily meteorological data sampled every 15 min on rainfall (mm), temperature (°C), and relative humidity (%) were obtained from the Haiti Regeneration Initiative rain gauge and weather station located in Port a Piment, Sud Department, Haiti (Fig. 1, open blue circle). Meteorological data were aggregated to represent cumulative daily totals for rainfall, and daily averages for temperature and relative humidity, from November 18, 2010 to December 26, 2011 (shown in Fig. 2).

National Aeronautics and Space Administration Precipitation Data. Satellite estimates of daily precipitation were obtained from the National Aeronautics and Space Administration (NASA) Tropical Rainfall Measuring Mission (TRMM), which provides area-averaged rainfall estimates at resolutions of $0.25^\circ \times 0.25^\circ$ from January 1, 1998 through June 30, 2011 (National Aeronautics and Space Administration). To estimate rainfall corresponding to the HAS case data, we used a $0.25^\circ \times 0.25^\circ$ square centered on HAS coordinates [19.074394, −72.491035], shown as shaded blue square in Fig. 1), which encompasses the primary HAS coverage area. Average rainfall nationwide was estimated using a latitude range [18.041N, 19.844N] and longitude range [74.323W, 71.79W], which inscribes a rectangle covering Haiti.

Modeling approaches

Statistical modeling

Distributed lag non-linear models of rain and cholera. Distributed lag nonlinear models (DLNM, Gasparrini et al., 2010) are a flexible statistical modeling approach built to account for a nonlinear relationship with delays between exposures and their effects. For a time series of outcomes Y_t with $t = 1, \ldots, n$, the general form of the model is given by:

$$g(\mu_t) = \alpha + \sum_{j=1}^{J} s_j(x_j; \boldsymbol{\beta}_j) + \sum_{k=1}^{K} \gamma_k u_{tk}$$

where $\mu = E(Y)$, g is a monotonic link function and Y is assumed to come from a distribution in the exponential family (Gasparrini

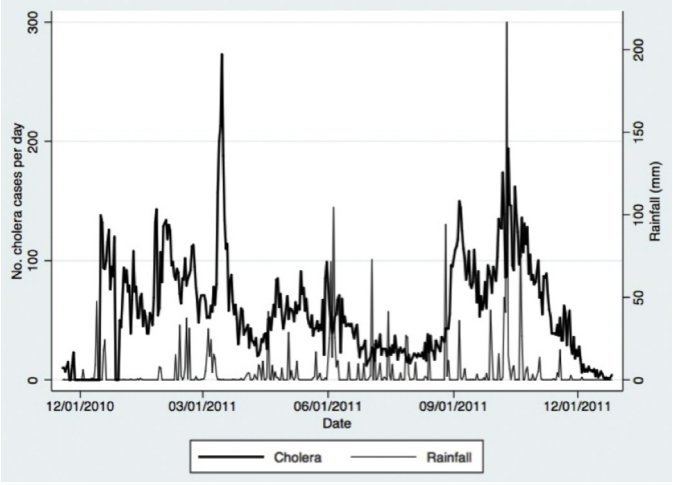

Fig. 2. Time plot of the number of cholera cases per day and daily cumulative rainfall (mm) in the Sud Department of Haiti, November 2010 to December 2011.

et al., 2010). The s_j's are smoothed functions of the exposure variables x_j (with parameters $\boldsymbol{\beta}_j$), belonging to a two-dimensional space of *cross-basis functions* that account for both the range of values and range of possible lags/delays in the effects of x. These basis functions are often taken to be polynomials or spline functions, to allow them to account for nonlinear relationships between the exposure (in this case rainfall) and effect (cases). The variables u_k represent other predictors, with linear effects given by the coefficients γ_k. A key concept in DLNMs is that of *harvesting*, which occurs when a predictor primarily affects a sub-group of individuals, causing their events (cases of cholera) to be shifted forward in time relative to the rest of the population. The depletion of this group from the population can then cause a subsequent reduction in cases (e.g. due to exhaustion of susceptibles from within this subgroup).

A DLNM was used to evaluate the association between precipitation and occurrence of cholera cases in Sud Department, using MSPP Sud case data and Port a Piment rain gauge data (described above). First-degree polynomials were used as basis functions for rainfall, and third-degree polynomial basis functions were used for the lag. To completely capture the overall rainfall effect and adjust for any potential harvesting (e.g. rainfall-related excess of cholera cases followed by deficits), we used lags up to 21 days. We controlled for daily temperature, relative humidity, and chronological study week in our model (by including these as covariates in our preliminary analysis). This forms a generalized linear model using the quasi-Poisson distribution that includes both the crossbasis for rain, as well as the variables temperature, relative humidity, and series week. Zero millimeters of rain was defined as the baseline rainfall (centering value) for calculating the relative risks.

Granger Causality Wald Test. The Granger causality Wald test was used to determine whether rainfall could be used to forecast peaks in cholera infections. The Granger causality Wald test is a method of using lags to test whether one time series can cause/predict another. A causal exposure to an independent variable should be associated with a lagged change in the dependent variable, and this relationship should be absent when the temporal sequence of exposure and response is reversed (Kuster et al., 2011). All analyses were performed using Stata (version 12.1; Stata Corporation) and R (version 2.14.1; The R Foundation for Statistical Computing).

Case Crossover Analysis. The case crossover approach is an epidemiological method for examining how short-term exposures (in this case rainfall) can cause transient changes in risk (in this case cholera risk), in which an individual serves as their own control (Maclure, 1991). This self-matching approach can allow one to consider situations where it can be difficult to recruit appropriately matched controls. Case crossover analysis was used to evaluate the relationship between rainfall estimates through the NASA TRMM and cholera cases seen at HAS (described above). We used a time-stratified 2:1 matched case-crossover design with hazard periods identified as the date of admission to HAS. Person-time at risk was divided into 3-week strata beginning on September 1, 2010. Control periods were the two days within each stratum that could be matched to the hazard period by day of the week and could precede, follow, or both precede and follow the hazard period. Estimates of plausible effect periods were based on a usual incubation period of 3–5 days for cholera (Kaper et al., 1995; Nelson et al., 2009). Aggregate rainfall exposures were defined as "likely during incubation" if they occurred 0–3 days before onset of disease, as "likely preceding incubation" if they occurred 4–7 days before onset of disease, or as "preceding incubation" if they occurred 8–11 or 12–15 days before onset of disease. Odds ratios (ORs) for occurrence of cases, based on rainfall effects, were approximated through the construction of a conditional logistic regression model.

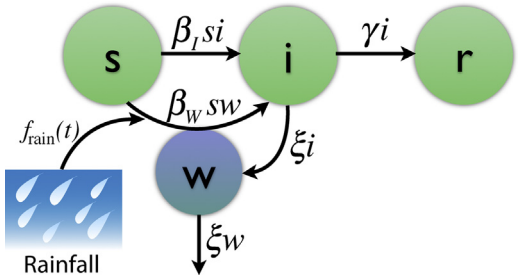

Fig. 3. Flow diagram for the scaled SIWR model with rainfall forcing (details on the model scaling given in Tien and Earn, 2010).

We assessed the dose–response relationship between rainfall and cholera case occurrence by assigning within-stratum (i.e. within a 3-week period) quintile ranks to our rainfall variable and incorporating the resulting estimates into regression models, both as dummy variables and as a 5-level ordinal variable. Evidence for a linear dose–response relationship was assessed using the Wald test for trend. All analyses were performed using Stata (version 12.1; Stata Corporation).

Dynamic modeling

We used the "susceptible-infectious-water-recovered" (SIWR) model of Tien and Earn (2010), which has been used previously in modeling cholera in Haiti (Tuite et al., 2011), as well as other contexts, including epidemic and endemic cholera in Angola and London (Tien et al., 2011; Eisenberg et al., 2013). This model is based on the classic "susceptible-infectious-recovered" model (Anderson and May, 1991), with an additional compartment representing concentration of pathogen in the water. The SIWR model contains two transmission pathways: a waterborne pathway (β_W) and a direct pathway (β_I). Note that the mathematical distinction between these two pathways is the timescale of transmission (see Tien and Earn, 2010 for analysis and further discussion), with the waterborne pathway representing a slower/delayed pathway. Previous studies have shown the need for including multiple timescales of transmission for modeling cholera dynamics (Tien et al., 2011; Eisenberg et al., 2013).

The scaled form of the model is shown in Fig. 3, where s represents the fraction of the population which is susceptible, i the fraction infected, and r the fraction of the population which is recovered/removed. The w compartment represents the concentration of pathogen in the water, scaled to the pathogen shedding and decay rates (details on the scaling are given in Tien and Earn, 2010).

Additionally, β_W is the transmission parameter for waterborne transmission, β_I the transmission parameter for direct transmission, γ the recovery/removal rate, and ξ the pathogen decay rate in the water. Note that ξ appears in the shedding term of the model due to the rescaling of the model given in Tien and Earn (2010), which eliminates the shedding rate parameter and makes the parameters identifiable (estimate-able) from case data (Eisenberg et al., 2013).

To account for the effects of rainfall on cholera transmission, we modified the waterborne transmission term, $\beta_W sw$, to include a rainfall data forcing function, denoted $f_{rain}(t)$. This incorporates a mechanistic connection between the environment, rainfall, and cholera disease dynamics. We take $f_{rain}(t)$ for a given rainfall data set to the be linear interpolation of the rainfall data points (though very similar results are obtained using other interpolation methods, e.g. cubic splines). Note that as $f_{rain}(t)$ is unnormalized, β_W and β_I are not directly comparable – for proper comparison,

β_W should be multiplied by the magnitude of the rainfall. The full model equations are thus:

$$\begin{aligned}\dot{s} &= -\beta_W s w f_{rain}(t) - \beta_I s i \\ \dot{i} &= \beta_W s w f_{rain}(t) + \beta_I s i - \gamma i \\ \dot{w} &= \xi(i - w) \\ \dot{r} &= \gamma i \\ y &= ki,\end{aligned} \tag{1}$$

where the equation $y = ki$ is a measurement equation indicating that we take the data to be given by a fraction k of the infected population, where k incorporates the reporting rate, infectious period, and total population size (see Eisenberg et al., 2013 for details). This is an approximation to the empirical hospitalization and treated case data considered here. We show in Eisenberg et al. (2013) that parameters for an SIWR model can be identified from this measurement equation, and thus use it here. To connect the noiseless measurement equation y with data, we assume each data point $z(t_i)$ is drawn from an independent Poisson random variable with mean $y(t_i)$. Model parameters were estimated for four regions/spatial scales, each paired with associated rainfall data for the region:

- HAS case data using NASA rainfall data for the HAS region in Deschappelles
- IDP camp case data using USGS rainfall data in the Port au Prince region
- Port au Prince MSPP case data using USGS rainfall data in the Port au Prince region
- Country-wide MSPP case data using NASA rainfall data for all of Haiti

The time spans considered were based on data availability, together with the constraint of being a sufficiently short time span such that vital dynamics and loss of immunity could be neglected. Both USGS rain gauges are in a similar spatial location (southeast of Port au Prince), so we tested both rain gauges for the IDP camp case data and the Port au Prince MSPP case data, as well as testing the corresponding TRMM rainfall data for Port au Prince (using a $0.25^\circ \times 0.25^\circ$ averaged area as in the other TRMM data sets). For comparison, model parameters were also estimated without any rainfall forcing (i.e. using the model as given in Eq. (1) with $f_{rain}(t) = 1$). In all cases, γ was fixed to 0.25, corresponding to an infectious period of 4 days, based on Weil et al. (2009) and WHO (2011). The initial condition for the infectious compartment ($i(0)$) was fitted to data, with $s(0) = 1 - i(0)$, and $r(0)$ taken to be 0 (noting that as there are no loss of immunity or birth/death processes, any initial recovered individuals will not affect the model dynamics). The initial condition for the environmental reservoir ($w(0)$) was fixed at 0.01. Parameters and initial conditions were estimated using maximum likelihood assuming Poisson distributed data with mean given by the measurement equation $y = ki$. Optimization was done using the Nelder–Mead algorithm with the function *fminsearch* in the software MATLAB. As a preliminary test of the predictive ability of the model, the model was also fitted to truncated data, where the last two, three, or four weeks of data were removed. In each case, the resulting models were then used to generate rainfall-forced predictions which were compared to the remaining case data points not used in fitting the model.

Results

Statistical modeling

Distributed Lag Non-Linear Models of Rain and Cholera. Summary statistics of daily weather conditions in Port a Piment and cholera case counts in Sud are given in Table 1. Although most days had no rain, the range was quite wide.

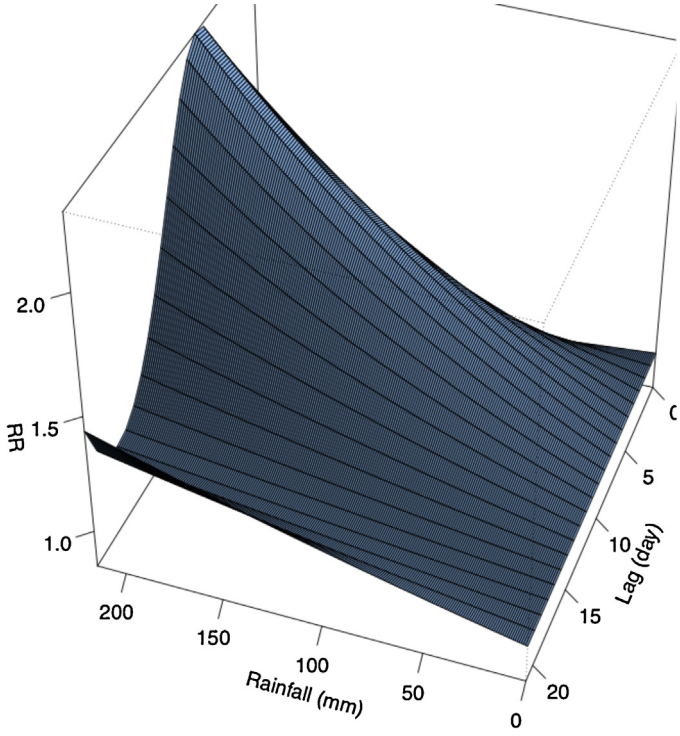

Fig. 4. Relative risks (RR, the ratio of cholera risk for individuals with a given rainfall exposure to the risk when unexposed) of cholera by daily cumulative rainfall (mm) over 21 days using a distributed lag nonlinear model (DLNM).

Fig. 4 shows the estimated relationship between rainfall, time lag, and relative cholera risk according to the DLNM fit. Increasing amounts of rainfall was associated with increased risk of cholera. This effect was delayed, with the maximum effects of heavy rainfall reached at a lag of approximately six to seven days. The effect of heavy rainfall on cholera risk was attenuated with lags of greater than seven days.

Fig. 5 shows cross-sections of the two-dimensional surface in Fig. 4, for fixed time lags (three, seven, and 14 days; left column) and daily rainfall totals (20,60 and 100 mm; right column). Again we can see that for any given lag, more rainfall increases the risk of cholera. This association is most pronounced at a lag of seven days. Additionally, for a given amount of rainfall, the risk of cholera consistently peaks between six and seven days of lag. The remaining variables controlled for (daily temperature, relative humidity, and chronological study week) did not show a significant relationship with cholera cases.

Granger Wald Causality Test. Peaks in rainfall appeared to precede unusual spikes in cholera cases, especially near the end of the time-series (September–November 2011). Based on the Granger causality Wald test, there is evidence that rainfall Granger-causes cholera disease (Chi-square = 34, df = 21, P = 0.035). Conversely, cholera disease could not be shown to Granger-cause rainfall (Chi-square = 16, df = 21, P = 0.79).

Case Crossover Analysis. A total of 4662 patients with cholera were seen at HAS between October 17, 2010 and July 11, 2011. The average age of patients was 31.4 years (SD = 22.0), 51.3% of which were male. The majority of patients lived in the Belanger (19.2%), Bastien (16.8%), or Liancourt (12.4%) sections within Verrettes Commune.

Increased occurrence of cholera was associated with cumulative precipitation >30 mm in the period that likely preceded infection (i.e., 4–7 days before occurrence of cases) (Fig. 6). The odds ratio (OR,

Table 1
Summary statistics of daily weather conditions from November 20, 2010 to June 4, 2011, in Port a Piment, Haiti as well as cholera for the Sud Department.

Variable	Minimum	25%	Median	75%	Maximum	Mean ± SD
Rainfall (mm)	0	0	0	1.6	216.7	4.8 (16.3)
Temperature (°C)	23.3	25.2	26.5	28.2	31.4	26.8 (2.0)
Relative humidity (%)	61.7	72.6	77.0	81.9	97.3	77.0 (7.1)
Cholera	0	26	52	84	273	58 (42)

SD, standard deviation.

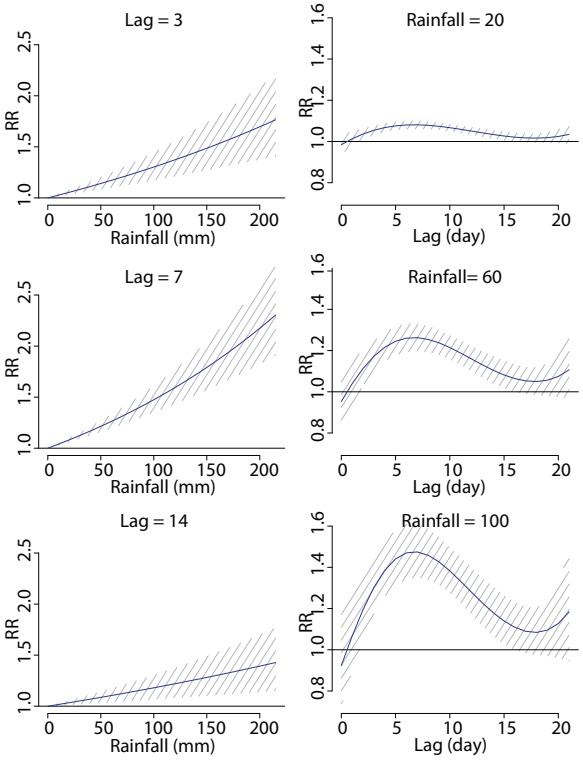

Fig. 5. Lag- and rainfall-specific relative risk of cholera. Hashed ribbons indicate the 95% confidence intervals.

ratio of odds of cholera with exposure to a particular level of rainfall at a given lag vs. without exposure) for cholera 4–7 days after rainfall was 1.46 (95% CI: 1.32, 1.61). Cholera was not associated with precipitation >8 days before occurrence of cases. Interestingly, the OR for cholera 0–3 days after rainfall was 0.64 (95% CI: 0.58, 0.71). The possibility of a dose–response relationship with rainfall was evaluated using a 4–7 day effect period. A positive dose–response relationship was seen for rainfall (Table 2).

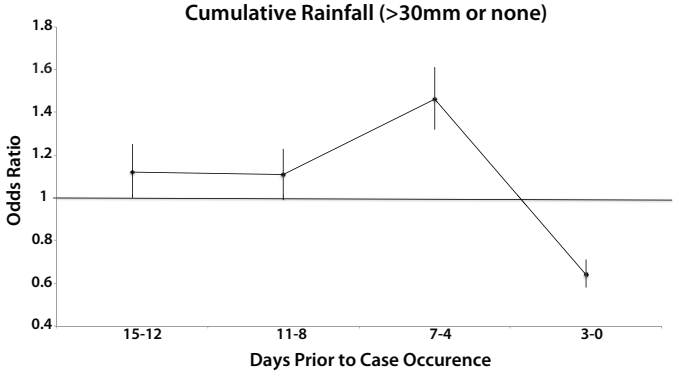

Fig. 6. Daily rainfall and risk of cholera in patients admitted to HAS. Error bars indicate the 95% confidence intervals, and the odds ratios are for >30 mm of rain vs. no rain.

Dynamic modeling

Model fits and parameter estimates using rainfall forcing are given in Fig. 7 and Table 3. Model fits using the rainfall data forcing function matched case data well, with relatively small residuals compared to the data magnitude (average absolute residuals were 22.7, 17, 119.9, and 741 for the HAS, IDP camp, Port au Prince, and national data sets, respectively). Similar fits were obtained with each of the USGS rain gauges, as well as with the TRMM Data, with the best fit rain data used in Fig. 7 and Table 3 (Morne Gentilehomme rainfall was used with the IDP camp case data, and Foret de Pins rainfall was used with the MSPP Port au Prince case data). Fits for the HAS and MSPP data (which include case data from the first weeks of the outbreak) were improved by dropping the first 3–5 data points (as shown in Fig. 7). The model fits without rainfall forcing were significantly worse than those with rainfall forcing and uniformly poor (fits not shown).

Model parameters were fairly consistent across different spatial settings (Table 3), though environmental and population size parameters β_W and k varied more significantly across different locations, as might be expected due to differences in rainfall/climate, population, surveillance, etc. Particularly notable is the much larger value of k (the proportionality parameter for the case count measurement) for HAS compared with Port-au-Prince. This suggests either a larger effective population size or reporting rate for HAS than Port-au-Prince (in spite of the larger population size of the latter). This is likely due to practical identifiability issues between $i(0)$ and k, wherein these two parameters can approximately compensate for one another. Fixing $i(0)$ to an order of magnitude larger ($i(0) = 0.0046$) and re-fitting the parameters results in extremely similar fits to the data and similar estimates for the other parameters, but with k reduced by an order of magnitude to compensate ($k^{-1} = 1.546 \times 10^{-5}$).

In most simulations, almost all transmission is due to the indirect pathway, with over 95% of incidence due to waterborne transmission throughout the simulations for the IDP camp, Port au Prince, and national-level data sets. However, for the HAS data set, the fraction of transmission does switch to being dominantly due to the direct pathway during the portion of the simulation where the data shows very few cases being generated (with ~80% of incidence due to direct transmission from Feb 6, 2011 through May 29, 2011). During this period the overall incidence data are quite small (averaging <20 cases per week, the smallest of all the data sets considered here), so this may be a function of the size of the

Table 2
Dose–response relationship between rainfall and risk of cholera in patients admitted to HAS. A 4–7-day effect period was used.

Precipitation quintile	OR (95% CI)[a]
1st (referent)	1
2nd	1.04 (0.91–1.17)
3rd	1.14 (1.01–1.28)
4th	0.87 (0.77–1.51)
5th	1.34 (1.19–1.51)

CI, confidence interval; OR, odds ratio.
[a] Wald χ^2, 10.29 (1 df); $P = 0.001$, test for linear trend.

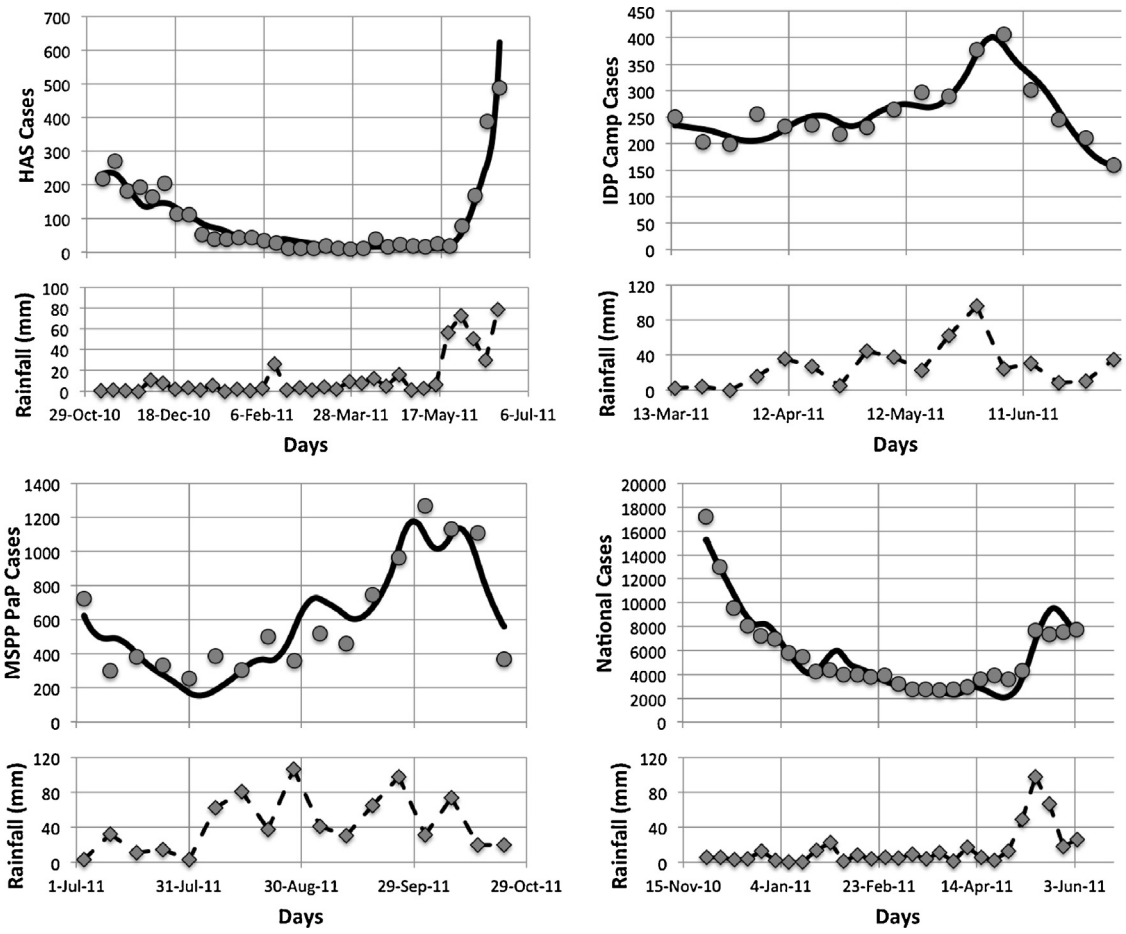

Fig. 7. Model (solid line) fits to data (circles) for each site using the rainfall forcing function (dashed line) generated from weekly rainfall data (diamonds). Clockwise, the panels are: HAS case data with NASA rainfall data, IDP Camp case data with USGS rainfall data from Morne Gentilehomme, Port au Prince (PaP) MSPP case data with USGS rainfall data from Foret de Pins, national MSPP case data with NASA rainfall data.

data. The pool of susceptibles is not strongly depleted, with >75% of susceptibles remaining at the end of the simulations for all four data sets.

The model predictions of case data were fairly accurate (with similar trajectories to the estimated models in Fig. 7), although the deviations between the predictions and the data increased as longer forecasting periods were considered, as shown in Fig. 8. While the national case predictions did yield a significant increase in cases in the last weeks of the simulation, the national predictions were less accurate than those done on a local/regional scale, and also deteriorated more noticeably as the prediction time-period increased. This might be expected as rainfall patterns vary widely across Haiti, and the national-level rainfall data also included some ocean rainfall (as this was within the rectangle inscribed around Haiti). For national case counts, a case count-weighted average of the local or departmental averaged rainfall may be more appropriate than the area averaged NASA rainfall data used here.

Discussion

This study quantitatively examines the relationship between rainfall and cholera incidence in Haiti on several different spatial scales, using a combination of statistical and dynamic modeling approaches. In all cases we find a strong relationship between rainfall and cholera, regardless of the methodology or spatial scale employed. Moreover, both approaches support a causal link between rainfall and cholera. Conclusions drawn from this type of multi-faceted approach may be more strongly supported than those using a single method, as they are less likely to be artifacts of the particular assumptions associated with a specific model. This also provides an opportunity to compare these different tools and examine how they may provide complementary information.

Time lags were either explicitly (in the case of the statistical models) or implicitly (dynamic models) incorporated into the analysis. Increased rainfall was associated with increased cholera

Table 3
Scaled SIWR parameter estimates fitted to weekly case data with rainfall forcing functions as shown in Fig. 7.

Parameter	Units	Description	Parameter Estimates			
			HAS	IDP Camp	PaP	National
β_I	days^{-1}	Direct transmission	0.212	0.243	0.155	0.214
β_W	days^{-1} mm^{-1}	Environmental transmission	0.00432	0.00128	0.00292	0.00108
ξ	days^{-1}	Pathogen decay rate	0.196	0.111	0.185	0.00958
k^{-1}	people^{-1}	Measurement scaling factor	1.92×10^{-6}	2.93×10^{-5}	1.39×10^{-5}	3.02×10^{-7}
$i(0)$	people	Initial condition for infected	0.00046	0.0069	0.0087	0.0046

PaP = Port au Prince.

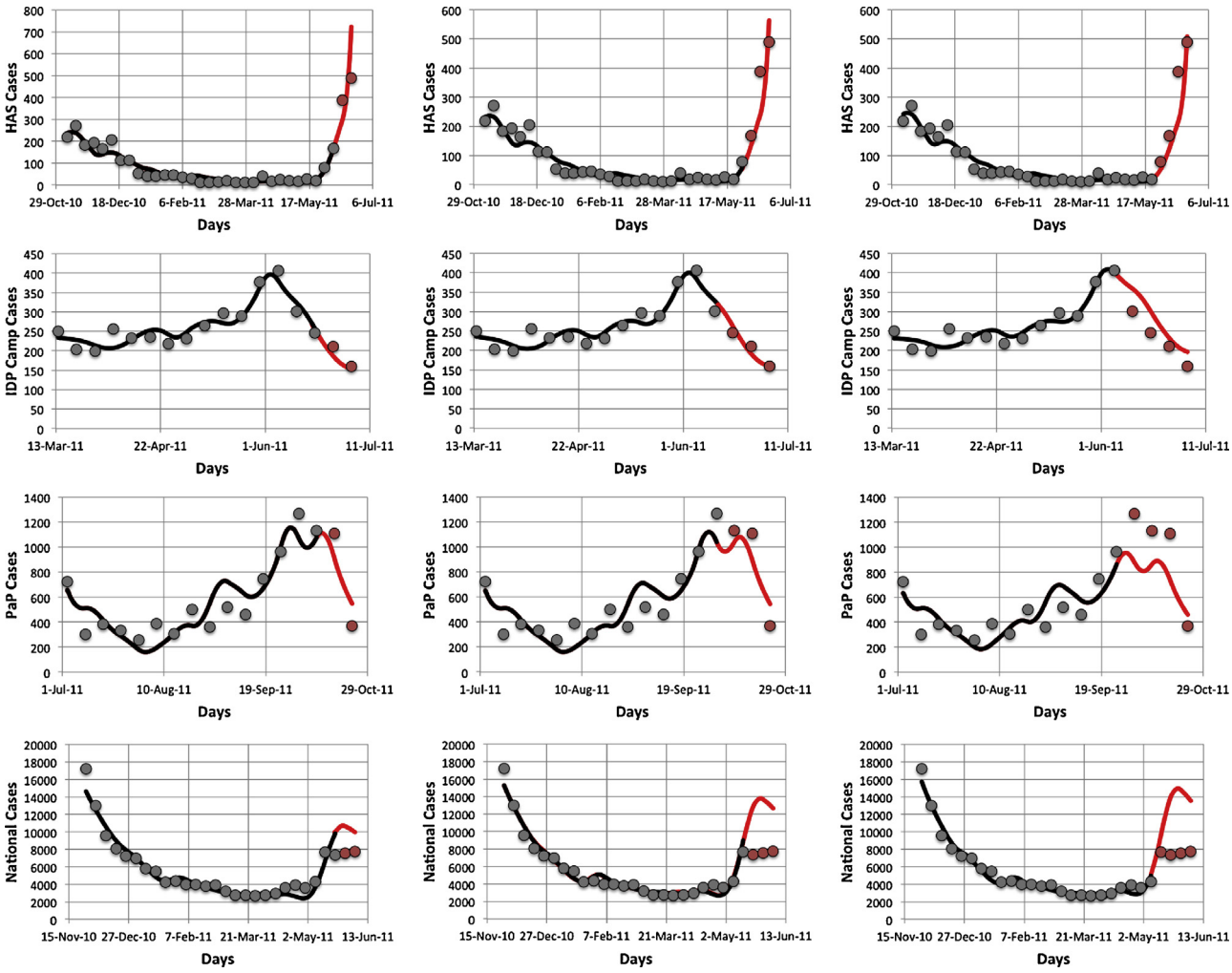

Fig. 8. Model fits (black line) to shortened case data (gray circles) with the last two (leftmost column), three (center column), or four (rightmost column) data points dropped. Subsequent model predictions compared to data points not used for fitting shown in red. Data sources are, from the top row to bottom row: HAS data, IDP Camps data, MSPP Port au Prince (PaP) data, and MSPP national case counts.

risk 4–7 days later. This lag is shorter than lags reported in endemic settings, which range from several weeks to 2 months (Emch et al., 2008; Hashizume et al., 2008, 2010; Mendelsohn and Dawson, 2008). This difference in time scale may reflect different environmental reservoirs for cholera bacteria in epidemic and endemic settings. Longer lags would be expected in settings where *V. cholerae* in estuarine or marine environments drive disease transmission through plankton blooms. Rainfall must first drive a plankton bloom (for example, through nutrient run-off) before a surge in cholera cases occurs. The short lag we report in the context of the current Haitian cholera epidemic may reflect abundant cholera bacteria in raw sewage. Given the lack of sanitation infrastructure currently in Haiti, heavy rains would cause sewage to contaminate surface and groundwater that individuals rely on for drinking, bathing, and washing clothes. In this case, the lag between rainfall and increased cholera cases need only incorporate the time needed to wash sewage into the water source, and the incubation period of the disease (three to five days Kaper et al., 1995; Nelson et al., 2009). This latter situation is more likely in epidemic situations, whereas the former is likely in endemic settings. Indeed, Rinaldo et al. (2012) treat rainfall as a forcing term which introduces cholera bacteria into water sources via sewage run-off. We hypothesize that in newly invading situations, short lags between rainfall and cholera cases will generally be observed.

The fits from our rainfall-forced dynamic models to the case data (Fig. 7) illustrate how fluctuations in rainfall may be used to generate corresponding fluctuations in cholera cases. This provides further evidence of a causal connection between rainfall and cholera incidence for a wide range of spatial locations and scales, and also suggests that rainfall data may represent the missing ingredient needed to create models of the Haitian cholera epidemic that actually project disease incidence. We have previously published a model of the early phase of the epidemic, and while we were able to fit a model that reproduced cumulative case counts over time, we were unable to reproduce week-to-week fluctuations in disease incidence (Tuite et al., 2011). At a seasonal timescale, other authors have noted the difficulty of fitting the secondary summer peak in cases seen using models without environmental/seasonal variables (Abrams et al., 2012). Indeed, in the absence of forcing, the SIWR model can only exhibit either a single-peak epidemic curve, or exist at an endemic equilibrium. It is therefore unsurprising that the SIWR model fit poorly without rainfall forcing, given that the case data does not match either of these two scenarios.

Rainfall-forced model fits were improved by dropping the case data points from the first weeks of the outbreak. This may suggest that the initial weeks of the epidemic included an invading phase that did not depend as strongly on rainfall, or may have a stronger spatial component not reflected in this model. This may also reflect

the fact that surveillance, case definitions, treatment levels, and other parameters changed significantly during the initial weeks of the epidemic, so that a constant set of parameters may not have been sufficient to describe the data.

The model fits and preliminary predictions in Fig. 8 suggest that developing predictive forecasting tools based on dynamic models of cholera in Haiti together with local or regional case surveillance data and environmental measures such as rainfall (e.g. via rain gauges or satellite precipitation data) may be feasible, and could benefit policy-makers, hospitals, and aid groups. However, forecasting cholera incidence will require using forecasted rather than measured rainfall data (as was considered in the test case given here). As rainfall prediction is itself a challenging task, this requires further research.

More broadly, depending upon the time frame of interest and desired level of detail, vital dynamics, loss of immunity, and the degree of spatial coupling between locations are all considerations. Other modeling approaches linking rainfall to the force of infection are possible as well, such as having rainfall-driven pathogen shedding or decay due to washout, among others (e.g. as in Rinaldo et al., 2012). There are also many different forms one might consider for the effects of rainfall, such as a thresholded or saturating effect, or having baseline transmission which is enhanced by rainfall. Preliminary testing of some of these alternative approaches to linking rainfall to cholera dynamics (e.g. having rainfall directly force the water compartment) did not yield significantly different fits to the data, perhaps because the cycle between water transmission and shedding into the water couples these different effects quite tightly. As the direct and environmental transmission pathways in the SIWR model represent different time scales of transmission, one might additionally examine other alternatives such as driving the direct transmission with rainfall effects, or using an indirect transmission pathway which is decoupled from the i compartment (e.g. as in King et al., 2008). Additional seasonal drivers such as flooding indices (e.g. as in Reiner et al., 2012) may also be useful to consider. The simple proportional relationship for rainfall in the waterborne transmission pathway used here highlights the strength of the relationship between rainfall and cholera; however further investigation of these different forms for the model would be productive, particularly as a wider range of environmental conditions, spatial scales, and locations are explored.

The relative ease with which the Haitian cholera epidemic is modeled when rainfall is included highlights the need for collection of basic rainfall data from across the country. Systematic collection of rainfall using rain gauges has not been a priority following the January 2010 earthquake. For the 2010–2011 period, to our knowledge reliable rainfall estimates from on-the-ground collection sites only exist for Sud and Port-au-Prince. The remote sensing rainfall estimates used here from NASAs Tropical Rainfall Measurement Mission are available at a resolution of $0.25^\circ \times 0.25^\circ$. Given Haiti's mountainous terrain, rainfall may vary significantly within this spatial resolution. On the other hand, USGS rain gauge data from Morne Gentilehomme resulted in excellent fits to cholera cases reported in the IDPs, despite the relatively large geographic distance of this gauge site from the camps (although this may also depend on the correlation scale of the rainfall pattern). Further study of how model estimates and predictions vary depending upon the spatial resolution of the rainfall data is needed.

Our findings also highlight the continued need for resources to combat cholera in Haiti. Many donors, aid organizations, and relief workers have worked to provide the IDPs with clean water following the earthquake. Perhaps due to these efforts, the IDPs were largely spared of cholera in 2010, despite Port-au-Prince being severely affected (Piarroux et al., 2011). However, the relative sparing of the IDPs, and the decline in cases country-wide by early 2011, created a false sense of security. The following rainy season brought a resurgence of disease across the country, including the IDPs. Past cholera outbreaks in camp settings elsewhere have been very severe, with the death of 12,000 Rwandan refugees in Goma as one tragic example (Siddique et al., 1995).

Cholera remains a serious concern for the IDPs, given the large number of Haitians still living in the camps combined with declining funding for NGOs supplying water and sanitation services (Butler, 2011). However, the IDPs are not alone in their need. Consider Hôpital Albert Schweitzer in the rural Artibonite Valley, whose 130 beds serve more than 340,000 individuals (Ernst et al., 2011). Closures of cholera treatment centers in the region puts an increased strain on facilities such as HAS which are already at capacity. There is the continued need to understand the factors affecting case load at the places where treatment occurs, and to ensure that sufficient resources are provided for care.

The quantitative link between rainfall and cholera presented here provides a framework for understanding cholera dynamics in Haiti on a longer time scale. Understanding cholera seasonality will be important for marshaling sufficient resources to deal with fluctuations in case loads, and for timing interventions to have their maximal effect (Earn et al., 1998). Conversely, interventions such as vaccinations can result in marked changes in disease seasonality (Earn et al., 2000), highlighting the need for quantitative model development. The results given here are focused on relatively short-term dynamics, and expanding the timescales considered in these models and data may be valuable both for intervention planning and for understanding the still-evolving long-term seasonal dynamics of cholera. Cholera poses several specific challenges in this regard: infectivity of cholera bacteria varies with how long ago the bacteria was shed, with freshly shed *V. cholerae* exhibiting "hyperinfectivity" (Alam et al., 2005; Merrell et al., 2002); microbial dose response curves (Haas et al., 1999) suggest nonlinear incidence functions which may alter disease dynamics (e.g. nonlinear incidence can give rise to disease oscillations even in the absence of environmental drivers, as explored analytically and by simulation in Dunworth (2011)); and the length of immunity may be associated with the severity of infection, and in general is not well understood (King et al., 2008). Furthermore, serotype switching by bacterial strains occurs as cholera epidemics progress. This has been the case in Haiti with recent identification of O1 strain-Inaba serotype-El Tor biotype bacteria (as distinct from the O1-Ogawa-El Tor strains that caused the initial outbreak) (Centers for Disease Control, 2012). As population-level immunity is a key determinant of disease dynamics, immune surveillance is potentially a valuable adjunct to traditional disease surveillance efforts for cholera. We note that hospital records on cholera patient re-admissions may be valuable for empirically estimating distributions of length of immunity. For example, HAS observed 67 repeat visits out of a total of 4662 cases from October 2010 to July 2011.

Our focus on rainfall is of course not intended in any way to deflect attention from the urgent need for sewage and water management infrastructure in Haiti, and indeed underscores this need. There are potentially other environmental drivers which are associated with cholera seasonality in endemic areas (Altizer et al., 2006; Constantin de Magny et al., 2008; Lipp et al., 2002). The seasonal oscillations resulting from the interaction of these different factors may not be obvious. For example, some of the Departments in Haiti showed a second peak in cholera cases in October 2011. This is reminiscent of seasonal patterns of cholera in Bangladesh, where some areas show one yearly peak in cases and other areas two peaks per year. Quantitative models can help us understand what seasonal patterns will emerge in different parts of Haiti as the disease becomes, as is likely, an established endemic pathogen. However, the work presented here shows that rainfall plays an important role for cholera in Haiti, and provides a foundation for

building predictive models of both short and long term cholera dynamics.

Acknowledgments

The authors are deeply grateful to Ian Rawson, Dawn Johnson, and Reynold Estime (HAS), as well as Patrick Duigan (IOM-Haiti) and Julio Urruela (WASH Cluster, Haiti UN) for their help and advice, including providing us with cholera case data from HAS and the IDP camps. We thank Mark Guseman (Ohio State University) for his assistance in obtaining the MSPP and rainfall data, and George Huffman (NASA Goddard) for valuable advice and assistance with the NASA TRMM data. This work was supported by the National Science Foundation through the Mathematical Biosciences Institute (DMS 0931642) and grant OCE-1115881 (to JT, ME, and DF). The images and data used in this study were acquired using the GES-DISC Interactive Online Visualization ANd aNalysis Infrastructure (Giovanni) as part of NASA's Goddard Earth Sciences (GES) Data and Information Services Center (DISC).

References

Abrams, J.Y., Copeland, J.R., Tauxe, R.V., Date, K.A., Belay, E.D., Mody, R.K., Mintz, E.D., 2012. Real-time modelling used for outbreak management during a cholera epidemic, Haiti, 2010–2011. Epidemiology and Infection, 1–10.

Adams, P., 2012. Haiti prepares for cholera vaccination but concerns remain. The Lancet 379 (9810), 16.

Alam, A., LaRocque, R.C., Harris, J.B., Vanderspurt, C., Ryan, E.T., Calderwood, Q.F.S.B., 2005. Hyperinfectivity of human-passaged *Vibrio cholerae* by growth in the infant mouse. Infection and Immunity 73 (10), 6674–6679.

Altizer, S., Dobson, A., Hosseini, P., Hudson, P., Pascual, M., Rohani, P., 2006. Seasonality and the dynamics of infectious diseases. Ecology Letters 9, 467–484.

Anderson, R.M., May, R.M., 1991. Infectious Diseases of Humans: Dynamics and Control. Oxford University Press, Oxford.

Bertuzzo, E., Casagrandi, R., Gatto, M., Rodriguez-Iturbe, I., Rinaldo, A., 2010. On spatially explicit models of cholera epidemics. Journal of the Royal Society Interface 7 (43), 321–333.

Bertuzzo, E., Mari, L., Righetto, L., Gatto, M., Casagrandi, R., Blokesch, M., Rodriguez-Iturbe, I., Rinaldo, A., 2011. Prediction of the spatial evolution and effects of control measures for the unfolding Haiti cholera outbreak. Geophysical Research Letters 38, L06403.

Butler, D., 2011. No quick fix for Haiti cholera. Nature 478 (October), 295–296.

Centers for Disease Control, 2012. Notes from the field: identification of *Vibrio cholerae* serogroup O1, serotype Inaba, biotype El Tor strain - Haiti, March 2012. Morbidity and Mortality Weekly Report (MMWR) 61, 309.

Chao, D.L., Halloran, M.E., Longini Jr., I.M., 2011. Vaccination strategies for epidemic cholera in Haiti with implications for the developing world. Proceedings of the National Academy of Sciences of the United States of America 108 (17), 7081–7085.

Chin, C.-C., Sorensen, J., Harris, J.B., Robins, W.P., Charles, R.C., Jean-Charles, R.R., Bullard, J., Webster, D.R., Kasarskis, A., Peluso, P., Paxinos, E.E., Yamaichi, Y., Calderwood, S.B., Mekalanos, J.J., Schadt, E.E., Waldor, M.K., 2011. The origin of the Haitian cholera outbreak strain. New England Journal of Medicine 364 (1), 33–42.

Constantin de Magny, G., Murtugudde, R., Sapiano, M.R.P., Nizam, A., Brown, C.W., Busalacchi, A.J., Yunus, M., Balakrish Nair, G., Gil, A.I., Lanata, C.F., Calkins, J., Manna, B., Rajendran, K., Mihir Kumar Bhattacharya, Huq, A., Bradley Sack, R., Colwell, R.R., 2008. Environmental signatures associated with cholera epidemics. Proceedings of the National Academy of Sciences of the United States of America 105 (46), 17676–17681.

Cravioto, A., Lanata, C., Lantagne, D.S., Nair, G.B., 2011. Final Report of the Independent Panel of Experts on the Cholera Outbreak in Haiti.

De Rochars, V.E.M.B., Tipret, J., Patrick, M., Jacobson, L., Barbour, K.E., Berendes, D., Bensyl, D., Frazier, C., Domercant, J.W., Archer, R., Roels, T., Tappero, J.W., Handzel, T., 2011. Knowledge, attitudes, and practices related to treatment and prevention of cholera, Haiti, 2010. Emerging Infectious Diseases 17 (11), 2158–2161.

Dunkle, S.E., Mba-Jonas, A., Loharikar, A., Fouche, B., Peck, M., Ayers, T., Archer, W.R., De Rochars, V.M.B., Bender, T., Moffett, D.B., Tappero, J.W., Dahourou, G., Roels, T.H., Quick, R., 2011. Epidemic cholera in a crowded urban environment, Port-au-Prince, Haiti. Emerging Infectious Diseases 17 (11), 2143–2146.

Dunworth, J.B., 2011. Nonlinear Incidence of Waterborne Diseases. Ohio State University, Master's thesis.

Earn, D.J.D., Rohani, P., Grenfell, B.T., 1998. Persistence, chaos and synchrony in ecology and epidemiology. Proceedings of the Royal Society of London Series B 265, 7–10.

Earn, David J.D., Rohani, P., Bolker, B.M., Grenfell, B.T., 2000. A simple model for complex dynamical transitions in epidemics. Science 287, 667–670.

Eisenberg, M., Robertson, S., Tien, J., 2013. Identifiability and estimation of multiple transmission pathways in waterborne disease. Journal of Theoretical Biology 324, 84–102.

Emch, M., Feldacke, C., Islam, M., Ali, M., 2008. Seasonality of cholera from 1974 to 2005: a review of global patterns. International Journal of Health Geographics 7.

Ernst, S., Weinrobe, C., Bien-Aime, C., Rawson, I., 2011. Cholera management and prevention at Hôpital Albert Schweitzer, Haiti. Emerging Infectious Diseases 17 (11), 2155–2157.

Faruque, S.M., Naser, I.B., Islam, M.J., Faruque, A., Ghosh, A., Nair, B.B., Sack, D.A., Mekalanos, J.J., 2005. Seasonal epidemics of cholera inversely correlate with the prevalence of environmental cholera phages. Proceedings of the National Academy of Sciences of the United States of America 102 (5), 1702–1707.

Fernandez, M.A.L., Bauernfeind, A., Jimenez, J.D., Gil, C.L., El Omeiri, N., Guibert, D.H., 2009. Influence of temperature and rainfall on the evolution of cholera epidemics in Lusaka, Zambia, 2003–2006: analysis of a time series. Transactions of the Royal Society of Tropical Medicine and Hygiene 103, 137–143.

Fisman, D.N., Lim, S., Wellenius, G.A., Johnson, C., Britz, P., Gaskins, M., Maher, J., Mittleman, M.A., Spain, C.V., Haas, C.N., Newbern, C., 2005. It's not the heat, it's the humidity: wet weather increases Legionellosis risk in the greater Philadelphia metropolitan area. Journal of Infectious Diseases 192, 2066–2073.

Gasparrini, A., Armstrong, B., Kenward, M.G., 2010. Distributed lag non-linear models. Statistics in Medicine 29, 2224–2234.

Gatto, M., Mari, L., Bertuzzo, E., Casagrandi, R., Righetto, L., Rodriguez-Iturbe, I., Rinaldo, A., 2012. Generalized reproduction numbers and the prediction of patterns in waterborne disease. Proceedings of the National Academy of Sciences of the United States of America 109 (48), 19703–19708.

Haas, C.N., Rose, J.B., Gerba, C.P., 1999. Quantitative Microbial Risk Assessment. John Wiley, New York.

Hashizume, M., Armstrong, B., Hajat, S., Wagatsuma, Y., Faruque, A.S.G., Hayashi, T., Sack, D.A., 2008. The effect of rainfall on the incidence of cholera in Bangladesh. Epidemiology 19 (1), 103–110.

Hashizume, M., Faruque, A.S.G., Wagatsuma, Y., Hayashi, T., Armstrong, B., 2010. Cholera in Bangladesh: climatic components of seasonal variation. Epidemiology 21 (5), 706–710.

Hill, V.R., Cohen, N., Kahler, A.M., Jones, J.L., Bopp, C.A., Marano, N., Tarr, C.L., Garrett, N.M., Boncy, J., Henry, A., Gomez, G.A., Wellman, M., Curtis, M., Freeman, M.M., Turnsek, M., Benner Jr., R.A., Dahourou, G., Espey, D., DePaola, A., Tappero, J.W., Handzel, T., Tauxe, R.V., 2011. Toxigenic *Vibrio cholerae* O1 in water and seafood, Haiti. Emerging Infectious Diseases 17 (11), 2147–2150.

Kaper, J.B., Glenn Morris Jr., J., Levine, M.M., 1995. Cholera. Clinical Microbiology Reviews 8 (1), 48–86.

King, A.A., Ionides, E.L., Pascual, M., Bouma, M.J., 2008. Inapparent infections and cholera dynamics. Nature 454, 877–880.

Koelle, K., Rodo, X., Pascual, M., Yunus, M., Mostafa, G., 2005. Refractory periods and climate forcing in cholera dynamics. Nature 436, 696–700.

Koelle, K., 2009. The impact of climate on the disease dynamics of cholera. Clinical Microbiology and Infection 15 (S1), 29–31.

Kuster, S.P., Tuite, A.R., Kwong, J.C., McGeer, A., The Toronto invasive bacterial diseases network, Fisman, D.N., 2011. Evaluation of coseasonality of influenza and invasive pneumococcal disease: results from prospective surveillance. PLoS Medicine 8 (6), e1001042.

Lipp, E., Huq, A., Colwell, R., 2002. Effects of global climate change on infectious disease: the cholera model. Clinical Microbiology Reviews 15 (4), 757–770.

Longini Jr., I.M., Yunus, M., Zaman, K., Siddique, A., Sack, R.B., Nizam, A., 2002. Epidemic and endemic cholera trends over a 33-year period in Bangladesh. Journal of Infectious Diseases 186, 246–251.

Maclure, M., 1991. The case-crossover design: a method for studying transient effects on the risk of acute events. American Journal of Epidemiology 133, 144–153.

MATLAB, Version R2010b. The MathWorks Inc., 2010.

Mendelsohn, J., Dawson, T., 2008. Climate and cholera in KwaZulu-Natal, South Africa: the role of environmental factors and implications for epidemic preparedness. International Journal of Hygiene and Environmental Health 211, 156–162.

Merrell, D., Butler, S., Quadri, F., Dolganov, N., Alam, A., Cohen, M., Calderwood, S., Schoolnik, G., Camilli, A., 2002. Host-induced epidemic spread of cholera bacterium. Nature 417 (6889), 642–645.

Ministere de la Sante Publique et de la Population, "Rapports journaliers du mspp sur l'évolution du choléra en haiti. http://www.mspp.gouv.ht/site/index.php?option=com_content&view=article&id=117&Itemid=1.".

National Aeronautics and Space Administration, "Rainfall archives: daily TRMM and other rainfall estimate (3B42 V6 derived). http://disc2.nascom.nasa.gov/Giovanni/tovas/TRMM_V6.3B42_daily.2.shtml".

Nelson, E.J., Harris, J.B., Glenn Morris Jr., J., Calderwood, S.B., Camilli, A., 2009. Cholera transmission: the host, pathogen and bacteriophage dynamic. Nature Reviews Microbiology 7, 693–702.

O'Connor, K.A., Cartwright, E., Loharikar, A., Routh, J., Gaines, J., Fouche, M.-D.B., Jean-Louis, R., Ayers, T., Johnson, D., Tappero, J.W., Roels, T.H., Archer, W.R., Dahourou, G.A., Mintz, E., Quick, R., Mahon, B.E., 2011. Risk factors early in the 2010 cholera epidemic, Haiti. Emerging Infectious Diseases 17 (11), 2136–2138.

Pascual, M., Rodo, X., Ellner, S.P., Colwell, R., Bouma, M.J., 2000. Cholera dynamics and El Niño-Southern oscillation. Science 289, 1766–1769.

Periago, M.R., Frieden, T.R., Tappero, J.W., De Cock, K.M., Aasen, B., Andrus, J.K., 2012. Elimination of cholera transmission in Haiti and the Dominican Republic. The Lancet 379 (9812), E12–E13.

Piarroux, R., Barrais, R., Faucher, B., Haus, R., Piarroux, M., Gaudart, J., Magloire, R., Raoult, D., 2011. Understanding the cholera epidemic, Haiti. Emerging Infectious Diseases 17 (7), 1161–1168.

R Development Core Team, 2012. R: A Language and Environment for Statistic Computing. R Foundation for Statistical Computing, Vienna, Austria.

Reiner, R.C., King, A.A., Emch, M., Yunus, M., Faruque, A.S.G., Pascual, M., 2012. Highly localized sensitivity to climate forcing drives endemic cholera in a megacity. Proceedings of the National Academy of Sciences of the United States of America.

Rinaldo, A., Bertuzzo, E., Mari, L., Righetto, L., Blokesch, M., Gatto, M., Casagrandi, R., Murray, M., Vesenbeckh, S.M., Rodriguez-Iturbe, I., 2012. Reassessment of the 2010–2011 Haiti cholera outbreak and rainfall-driven multiseason projections. Proceedings of the National Academy of Sciences of the United States of America 109 (17), 6602–6607.

Ruiz-Moreno, D., Pascual, M., Bouma, M., Dobson, A., Cash, B., 2007. Cholera seasonality in Madras (1901-1940): dual role for rainfall in endemic and epidemic regions. Ecohealth 4, 52–62.

Siddique, A., Salam, A., Islam, M., Akram, K., Majumdar, R., Zaman, K., Fronczak, N., Laston, S., 1995. Why treatment centers failed to prevent cholera deaths among Rwandan refugees in Goma, Zaire. The Lancet 345 (8946), 359–361.

StataCorp, 2011. Stata Statistical Software: Release 12. StataCorp LP, College Station, TX.

Tien, J.H., Earn, D.J.D., 2010. Multiple transmission pathways and disease dynamics in a waterborne pathogen model. Bulletin of Mathematical Biology 72 (6), 1506–1533.

Tien, J.H., Poinar, H.N., Fisman, D.N., Earn, D.J.D., 2011. Herald waves of cholera in 19th century London. Journal of the Royal Society Interface 8 (58), 756–760.

Tuite, A.R., Tien, J., Eisenberg, M., Earn, D.J., Ma, J., Fisman, D.N., 2011. Cholera epidemic in Haiti, 2010: using a transmission model to explain spatial spread of disease and identify optimal control interventions. Annals of Internal Medicine 154 (9), 593–601.

U.S. Geological Survey, "USGS 508332999940 Morne Gentilehomme raingage, Haiti. http://waterdata.usgs.gov/pr/nwis/uv?cb_00045=on&format=html&.=60&site_no=508332999940.".

U.S. Geological Survey, "USGS 508332999970 Foret de Pins raingage, Haiti. http://waterdata.usgs.gov/pr/nwis/uv?cb_00045=on&format=html&.=60&site_no=508332999970.".

Weil, A.A., Khan, A.I., Chowdhury, F., LaRocque, R.C., Faruque, A.S.G., Ryan, E.T., Calderwood, S.B., Qadri, F., Harris, J.B., 2009. Clinical outcomes of household contacts of patients with cholera in Bangladesh. Clinical Infectious Diseases 49, 1473–1479.

WHO, 2011. World Health Organization – Cholera Factsheet. http://www.who.int/mediacentre/factsheets/fs107/en/index.html